We are IntechOpen, the world's leading publisher of Open Access books Built by scientists, for scientists

6,900
Open access books available

185,000
International authors and editors

200M
Downloads

Our authors are among the

154
Countries delivered to

TOP 1%
most cited scientists

12.2%
Contributors from top 500 universities



WEB OF SCIENCE™

Selection of our books indexed in the Book Citation Index in Web of Science™ Core Collection (BKCI)

Interested in publishing with us?
Contact book.department@intechopen.com

Numbers displayed above are based on latest data collected.
For more information visit www.intechopen.com



Chapter 4

Mechanical Properties of Thermoelectric Materials for Practical Applications

Gilad M. Guttmann and Yaniv Gelbstein

Additional information is available at the end of the chapter

http://dx.doi.org/10.5772/intechopen.75476

Abstract

Thermoelectric (TE) direct conversion of thermal energy into electricity is a novel renewable energy conversion method currently at a technological readiness level of 3–5 approaching laboratory prototypes. While approaching practical thermoelectric devices, an increase in the thermoelectric element's efficiency is needed at the entire service temperature range. Yet, the main focus of research was concentrated on the electronic properties of the materials, while research on the mechanical properties was left behind. As it is shown in this chapter, knowing and controlling the mechanical properties of TE materials are paramount necessities for approaching practical TEGs. The material's elastic constants, strength and fracture toughness are the most crucial parameters for designing of practical devices. The elastic constants provide understanding about the material's stiffness, while strength provides the loading conditions in which the material will keep its original shape. Knowing the fracture toughness provides the stress envelope in which the material could operate and its susceptibility to inherent fabrication faults. The characterization methods of these properties are varied and may be physical or pure mechanical in nature. It is the authors opinion to prefer the mechanical methods, so the results obtained will describe more accurately the material's response to mechanical loading.

Keywords: thermoelectric applications, thermoelectric materials, TEG prototype, mechanical properties, fracture toughness

1. Introduction

The demand for clean and reliable energy-harvesting technologies over the past few decades has led researchers to focus much on thermoelectric power generation (TEG) techniques. The thermoelectric effects (namely Peltier and Seebeck effects) exhibit the ability of a material

IntechOpen

© 2018 The Author(s). Licensee IntechOpen. This chapter is distributed under the terms of the Creative Commons Attribution License (http://creativecommons.org/licenses/by/3.0), which permits unrestricted use, distribution, and reproduction in any medium, provided the original work is properly cited. CC BY

subjected to temperature gradient, to mobilize charge carriers within its volume. The right connection of two such materials can be used for building a TEG module which is reliable, quiet (due to no moving parts), and most importantly scalable. Such TEG modules had been used for the past 40 or so years as reliable power generators in top-edge technology systems at remote terrestrial and extra-terrestrial locations in NASA's systems. Furthermore, one can take advantage of the thermoelectric (TE) effects and tailor other types of modules for different applications, in a wide range of operating temperatures, such as cooling systems in cars (enhancing the coefficient of performance, COP, of the entire cooling system and car performance), harvesting residual heat from solar systems and photo-voltaic conversion cells, and harvesting residual heat from heat exchangers and converting it to useful electricity at industry, power supply modules for onsite sensor systems, and even wearable devices (if incorporated in organic films).

The energy conversion efficiency is a fraction of the Carnot efficiency and determined by the dimensionless figure of merit (ZT), which is defined as $ZT = \alpha^2 T/\rho\kappa$, where α, T, ρ, and κ are the Seebeck coefficient, absolute temperature, electrical resistivity, and thermal conductivity, respectively. While most of the research in the past 15 years was focused on improving the ZT of materials (and hence the efficiency), a little focus was given to the mechanical evaluation and reliability of these materials. Therefore, much work of evaluating the material properties in the mechanical, thermomechanical, and fatigue fields is still to be done while paying attention to the TEG whole-module integrity challenges such as thermal stability and metalized contact layer durability [1, 2].

From the physics standpoint both transport and mechanical properties originate at the atomic level. The mechanical response of the material mainly depends on the atomic bonding between the atoms from which it is constructed. An atomic bond is basically the sharing of electron(s) between two or more adjacent particles (nonmetals for covalent bond, ions for ionic bond, or atom nucleus for metals). The cohesive energy (E_C) between two particles is a measure of the work required for their separation and is a result of the repulsive and attractive forces between the two, which depend on the particle masses (the same force law as in gravity). The distance between two particles where the potential energy is minimal defines the cohesive energy of the two. The stronger the cohesive energy, the stronger the bond between the particles and more work is required for breaking the bonds. The gradient of force per small change of distance between the particles is defined as Young's modulus. The material strength is the force required to break atomic bonds and forcing a plastic and constant change in the material volume. The material compressibility, better known for its reciprocal—bulk modulus (B), is a measure for the material's resistance to hydrostatic compression. Many researchers tried over the years to find relations between the cohesive energy and bulk modulus to other various physical properties of the material (such as melting temperature, atomic volume, lattice constants, Debye temperature, etc.). Such specific connections will undoubtedly be restricted to a group of materials with similar structure, bond type, or other physicochemical property. Recently, after the examination of a large reported database on the physical properties of about 30 metals, it was realized that a correlation between the bulk modulus and the cohesive energy density (the atomic cohesive energy divided over the atomic volume—E_C/V) can be made [3]. Such a correlation opens the possibilities of correlating the other elastic constants

of the material including Young's modulus to other physical properties and therefore interlinking the material transport and electric properties with the mechanical ones on the atomic level.

The above long list of different suggested applications for TEGs is to show the wide range of service conditions that these generators will need to withstand. Such applications may vary from static operating conditions with a low number of thermal cycles and low operating temperatures, via higher temperature amplitudes and frequencies and up to dynamic applications with a high number of cycles, high thermal amplitudes, and occasional mechanical impacts.

Furthermore, the TEG service conditions necessarily subject the materials to wide temperature ranges and gradients within the materials themselves, so any mechanical characterization of TE materials should also concern the temperature dependence of the property. One such work was conducted measuring Young's modulus temperature dependence of LAST (Pb-Sb-Ag-Te) [4] between room temperature and 823 K and found an inverse relation between Young's modulus and the temperature.

In order to advance the development of thermoelectric modules for approaching practical applications, the design of future modules must take into account the mechanical properties of the involved materials for assuring adherence to the service conditions. Such design approaches based on finite element analysis, carried out for different applications, were reported [5–8]. Such analyses are essential while designing a specific TE device and give the ability to play with different parameters without the need of physical construction—saving money, time, man power, and materials in the process. Any simulation of the mechanical performance most definitely requires the values of the material's elastic constants (Young's, bulk, shear, Poisson's ratio) and strengths for the very least.

Measuring or evaluating correctly the mechanical properties of TE materials has the potential to bridge between the atomic (mechanical) and physical (electronic/transport) understanding of these materials to the fully developed working modules that will be optimal from both ends standpoint. That way, the material selection for the proper usage will be much easier and efficient.

Therefore, in order to achieve optimal operational TEGs, further evaluation and maximization of the following mechanical properties—elastic modulus, strength, hardness, fracture toughness, fatigue resistance (fatigue limit), and thermal fatigue resistance—are required at the entire operational temperature range (depending on the application). These are not the only mechanical properties at question but are the major ones that will provide both scientists and manufacturers with sufficient data to improve and further proceed to practical TEGs. As it will be clarified in detail, characterizing these few mechanical properties is handful enough for the time being.

2. Mechanical properties

All the mechanical property results for most of the currently investigated TE materials reported in this chapter are summarized in **Table 1** for convenience.

Material	Reference	Type	ZT_{max}	E sonic (GPa)	ν Poisson's ratio	E mechanical (GPa)	σ (MPa)	Hv (GPa)	K_I (MPa × $m^{1/2}$)	VIF constant
PbTe		p	0.8	27.7				0.41	0.35	
GeTe	—	p	0.8	57.0	0.27	77 (a)	168 (a)	1.16	0.39 (i)	0.0319
GeTe + 10% Ag	—	p	0.5	48.8	0.29	65 (a)	216 (a)	1.41	0.41 (i)	0.0319
GeTe + 10% Cu	—	p	0.7	60.7	0.26		239 (a)	1.59	0.44 (i)	0.0319
GeTe + 4% at Bi_2Te_3 + 10% Ag	—	p	0.7	49.4	0.28	59 (a)	221 (a)	1.58	0.48 (i)	0.0319
GeTe + 4% at Bi_2Te_3	—	p	0.6	47.8	0.26	79 (a)	176 (a)	1.62	0.54 (i)	0.0319
GeTe + 4% at Bi_2Te_3 + 10% Cu	—	p	0.7	62.7	0.25	63 (a)	204 (a)	1.78	0.56 (i)	0.0319
Zn_4Sb_3	[9]	p		71.7	0.26		56.6 (a)	2.2–2.3	0.8–1.2 (i)	0.016
$Si_{0.8}Ge_{0.2}$	[10]	n	0.9	143	0.23		86 (c)	14.5 (i)	1 (i)	0.0089
$Si_{80}Ge_{20}$	[11]	p				135 (b)	108 (c)	9 (i)	1.66 (i)	0.0089
Bi_2Te_3	[12]	n	1	32			62 (a)	0.62–0.79 (i)	1.1 (i)	unknown
Mg_2Si	[13]	n	1	117				5.3 (i)	1.25 (i)	0.016
$Yb_{0.35}Co_4Sb_{12}$	[14]	n	0.35–1	135	0.20		111	8 (i)	1.7 (i)	unknown
$Ca_3Co_4O_9$	[15]	p				84 (b)	320 (C)	2.6 (ii)	2.8 (iii)	
$CoSb_3$	[16]	n		136	0.14–0.25	92 (a)	766 (a); 86 (c)		1.7 (iii)	
$CeFe_3RuSb_3$	[16]	p		133	0.22–0.29	115 (a)	657 (a); 37 (c)		1.1–2.8 (iii)	
Bi_3Se_2Te	[17]					197.2 (b)		5.6 (ii)	2.4–2.6 (ii)	0.016
Bi_2Te_3	[18]	p			0.25	127.5 (b)		4.02 (ii)		
$Hf_{0.44}Zr_{0.44}Ti_{0.12}CoSb_{0.8}Sn_{0.2}$	[19]	p				221.0 (b)		12.8 (ii)		
$Hf_{0.25}Zr_{0.75}NiSn_{0.99}Sb_{0.01}$	[19]	n				186.5 (b)		9.1 (ii)		

Material	Reference	Type	ZT_{max}	*E* sonic (GPa)	*ν* Poisson's ratio	*E* mechanical (GPa)	*σ* (MPa)	*Hv* (GPa)	K_I (MPa × $m^{1/2}$)	VIF constant
$Bi_{0.4}Sb_{1.6}Te3$	[19]	*p*				41.5 (b)		1.1 (ii)		
$Bi_2Te_{2.7}Se_{0.3}$	[19]	*n*				38.8 (b)		1.2 (ii)		
$Ce_{0.45}Nd_{0.45}Fe_{3.5}Co_{0.5}Sb_{12}$	[19]	*p*				129.7 (b)		5.6 (ii)		
$Yb_{0.35}Co_4Sb_{12}$	[19]	*n*				136.9 (b)		5.8 (ii)		
$Si_{0.8}Ge_{0.2}P_2$	[19]	n				166.3 (b)		10.8 (ii)		
$Si_{0.8}Ge_{0.2}B_5$	[19]	*p*				155.6 (b)		10.7 (ii)		
$In_{0.005}PbSe$	[19]	*p*				65.9 (b)		0.6 (ii)		
$Bi_xSb_{2-x}Te$	[20]	*p*	1.4			42.1 (b)		1.6 (ii)		
$Ba_8Al_{15}Si_{31}$	[21]		0.4	96.88	0.25	109.7 (b)			1.1	0.018
MnSi	[22]	*p*	0.6			160(a); 182 (b)	1083 (a); 178 (c)	11.85 (i)	1.63 (i)	0.16
$Mg_2Si_{1-x}Sn_x$	[22]	*n*	1.1			83 (a); 58 (b)	492 (a); 79 (c)	3.54 (i)	0.99 (i)	0.16

(a) = compression; (b) = nanoindentation; (c) = flexural; (i) = Vickers Indentation Fracture; (ii) = nanoindentation; (iii) = other method from ASTM C 1421

ZT_{max} is the material's maximal figure of merit; *Esonic,* Young's modulus as measured by sonic method; ν, Poisson's ratio; *E mechanical*, Young's modulus as measured in a mechanical testing method; *σ*, maximum strength as measured by mechanical testing method; *Hv*, hardness Vickers; K_{VIF}, fracture toughness; VIF constant, the constant used in the Vickers Indentation Fracture equation to calculate the fracture toughness.

Table 1. Summary of the mechanical properties of various TE materials reported in the study.

http://dx.doi.org/10.5772/intechopen.75476

2.1. Elastic modulus

Young's modulus, frequently designated as E, is the most common and known member of a family of elastic constants that describe the elastic response of a material. Other constants are the shear modulus (G), Poisson's ratio (v), bulk modulus (B), and Lame's constant (λ). These constants are manifestation of the minimum free energy between the atoms that construct the material and therefore depend on the material's atomic composition and structure. They describe the elastic response of a solid to different imposed mechanical stresses and can be used as indicators of phase transition of the material with changing of temperature or pressure [23].

Young's modulus describes the material's elastic response to a uniaxial loading (either tension or compression) and gives the linear proportion of increase in the stress while increasing the displacement on the material. It is the same as with a spring's constant and obeys Hook's law (Eq. (1))

$$\sigma = E \cdot \varepsilon \tag{1}$$

where σ is the measured stress (Pa), E is Young's modulus (Pa), and ε is the displacement (mm/mm). So by studying the stress-strain curve of a material under uniaxial loading, the material's Young's modulus can be determined by measuring the initial linear slope of the curvature. As long as the material is subjected to stresses at the elastic range and do not undergo any plastic deformation, Young's modulus is a good indicator for the general stiffness of the material.

A different characterization technique of the elastic modulus is by measuring the time of flight of transverse and shear waves (see **Figure 1**) in a material (ASTM D 2845 [24]). This test method is good for estimating the elastic constants of the material—especially in the case of brittle nature materials or low-volume productions (where standard mechanical specimens for tensile/compression could not be fabricated). In contrast to mechanical testing where the

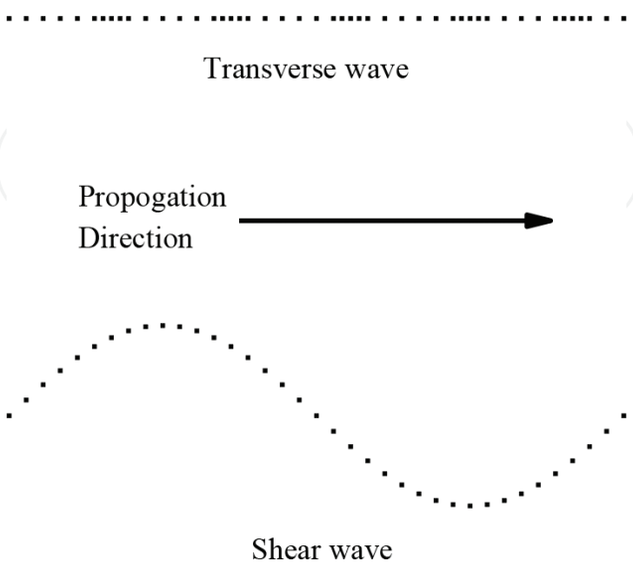


Figure 1. A schematic presentation of transverse and shear sound waves.

http://dx.doi.org/10.5772/intechopen.75476

elastic response of the material to applied external stresses is measured in the case of time of flight, the sound velocity of elastic waves propagation through (transverse) and along (shear) the material is being characterized.

Each sound wave is excited within the material by a piezoelectric transducer working in the ultrasonic range (above 20 kHz). Usually, the same transducer can excite and receive sound waves, and a record of the voltage as a function of time can be plotted. A repetitive pattern is recorded with a decreasing amplitude, due to inelastic interactions in the material (heat generation, absorption).

Measuring the time difference between identical points in the repetitive pattern and dividing it by the specimen geometry allow measuring the sound velocity (V_L for transverse wave and V_S for shear wave). Then, the elastic constants could be evaluated using the following equations[1] [24]:

$$E = \frac{\left[\rho V_s^2\left(3V_L^2 - 4V_s^2\right)\right]}{\left(V_L^2 - V_s^2\right)} \tag{2}$$

$$\nu = \frac{\left(V_L^2 - 2V_s^2\right)}{\left[2\left(V_L^2 - V_s^2\right)\right]} \tag{3}$$

where ρ is the material density (gr/m^3), E is Young's modulus (Pa), and ν is Poisson's ratio.

A comparison of Young's modulus values measured by the sonic and mechanical methods has shown that some difference in results (up to 30%) may exist [25, 26]. The sonic-based method is less prone and sensitive to internal defects within the material's volume (up to the case where such defects affect the measured sound velocity) than the mechanical method. From this, it can be concluded that the sonic evaluation of Young's modulus will be used to distinguish between different TE material systems, but mechanical values, which are more sensitive and indicative for the actual external stresses that will be applied upon the materials, will be more suitable for the mechanical design of modules and for comparing fabrication procedures.

Investigating the elastic modulus values of different TE materials reported in the study reveals that most of the TE materials exhibit values close to common engineering metals in the range of several tens of GPa and up to 200 GPa (for a comparison, ~70 GPa is characteristic for Al alloys and ~200 GPa for steels) [27, 28]. This fact can ease some of the concerns while modeling and designing of future TE devices, because the stiffness of the different materials is not poles apart from one another.

Bismuth telluride (Bi_2Te_3)-based TE alloys exhibit the lowest and highest reported elastic modulus values, as low as ~40 GPa and up to ~200 GPa, depending on the exact alloying and fabrication procedure [12, 18]. Lead telluride (PbTe)-based alloys (which is the most researched alloy system) exhibit modulus values of ~60 GPa [1]. More advanced and recent alloys such as

[1]Here, the calculations for Young's modulus and Poisson's ratio are brought. Calculations for the other elastic constants can be found at the ASTM standard [9].

skutterudites exhibit values of ~100 GPa [19], silicon germanium (SiGe)-based alloys exhibit values of ~150 GPa [10, 11, 19], and half-Heusler alloys can even reach ~200 GPa [19].

These values show the versatility of the material systems and research opportunities while involving different alloying and fabrication procedures, highlighting the major role of the involved materials at the mechanical design stage.

2.2. Strength

Strength is defined as the stress that the material can withstand under any loading condition before any permanent change is introduced to the material. It is common to differentiate between several specific strength definitions of materials (see **Figure 2**). The first is the *yield strength*, which is defined as the stress at which the material undergoes a uniform plastic deformation (most common in metals), which means that after the load is removed, the material will not regain its full initial shape. The second is the *ultimate strength*, which is the maximal stress that the material can withstand after which a plastic deformation becomes local at the weakest site in the material (for ductile materials). The third is the *fracture strength*, which is the stress at which all of the plastic deformation are exploited and defect in the material coalescence and concluded in a final fracture of the material. In the case of materials with a brittle nature, the ultimate strength usually coincides with the final fracture.

In order to measure the material's strength, one must subject it to external loading, preferably in only one axis. The most common test is the tensile test at which a specimen is held at the testing machine and the external forces elongate the specimen and further open any defect present in the material. Therefore, the tensile test is very sensitive to the specimen fabrication method and its associated defects.

On the other end, a compression test can be performed, at which the external forces act in the direction to decrease the volume of the specimen and to stop any propagation of defects

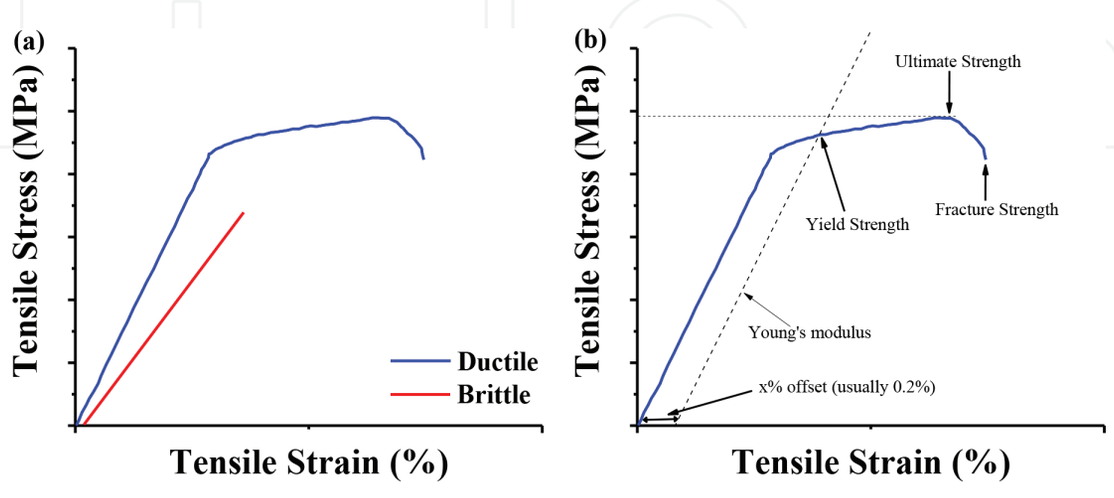


Figure 2. A schematic stress-strain curve: (a) ductile versus brittle material and (b) strength definitions.

in the material. The compression test is very common in the ceramics and semiconducting material classes in which minimization of the results deviation due to material's defects is significant.

Most TE materials are brittle in nature, meaning that their majority do not show any signs of plastic deformation (and therefore no yield strength), and fracture is rather catastrophic. Bi_2Te_3 and its alloys have the longest history of utilization for direct energy conversion, and hence their mechanical strength received early attention. Such ingots made by conventional zone-melting growth exhibited only 10–20 MPa flexural fracture strength [1]. A low mechanical strength of TE materials not only results in failure during element fabrication but also limits the degree of miniaturization which is required among others for TE modules for microelectronics [1]. Enhancing the material strength can be achieved by engineering the material microstructure in the micron and submicron scales. Furthermore, experiments were also made trying to incorporate nano-particles or wires for producing composite materials [13, 29]. The latter fabrication approach usually results in lower *ZT* of the materials with enhanced mechanical properties, which are associated with the strengthening components, without any significant contribution to the TE performance.

The reported fracture strength of most of the TE materials is in the range of 60–200 MPa, much depending on the testing method (lower values for the flexural test and higher values in the case of compression). Skutterudites and half-Heusler materials show the highest reported strengths in the range of 600–800 MPa [16, 17].

2.3. Hardness

Hardness is a material quality rather than a physical property (here to say that this value has no real meaning for itself, but only in a comparison to other materials or metallurgical states) that defines the material's resistance to penetration. There are several scales of hardness being used in materials science and engineering, where the most common are the ***Rockwell*** and ***Brinell*** scales usually used on metals and the ***Vickers*** scale that are also common in ceramics. The scales differ from each other by four parameters: (1) indenter geometry and compositions, (2) applied load during the test, (3) dwell time at maximal load, and (4) means of result interpretation. For instance, Rockwell hardness is determined using either a diamond cone indenter or a stainless steel ball (1/16″) under a load ranging from 15 to 150 kgf. The resulting hardness is a measure of the depth the indenter makes into the material. On the other hand, Vickers hardness is obtained by measuring the mean diagonals of an indent resulting by a square-based pyramid with a head angle of 136° made of diamond and loads ranging from several grams (micro-hardness) up to 120 kgf. Some overlap between the different scales can be found so a comparison could be made.

Notice that hardness is also an indicator for the material's resistance to wear. If the material is too soft, the surface is easily damaged during handling or device assembly.

Comparison made between hardness values obtained by micro-hardness and nano-indentation (further explanation in Section 2.4.2) found that the latter may result in 10–30% higher

values than the first, especially in materials exhibiting plasticity and has a low ratio of yield strength to Young's modulus. These conditions lead to a pileup of the plastically deformed surface at the edges of the indenter during the nano-indentation test, which in result make the affective contact area, between the indenter and the material's surface. The hardness result is determined by dividing the maximal applied force by the apparent contact area measured after the load has removed, without taking into account the pileup [30]. Therefore, nano-indentation values must be corrected in such cases. Later report comparing both of the techniques for a TE material (*n*-type LAST) [31] found that the values obtained by both of the techniques are in a very good agreement and in the range of 0.6–0.8 GPa. Such values (at the range of ~1 GPa) were reported for the most common TE materials at the early years (see **Table 1** at the beginning of the chapter). Higher values were reported more recently for different materials upon fabrication changes. SiGe and half-Heusler alloys were reported to exhibit a hardness of ~14 GPa [19].

2.4. Fracture toughness

Fracture toughness is the material's ability to adhere loading at the presence of inherent flaws before catastrophic failure will occur. For a brittle material (here to say without the ability for plastic deformation at the crack tip), the fracture toughness K_c (MPa·√m) reflects the flaw tolerance which is typically dependent on the preexisting flaw length, a_c(m), as indicated in Eq. (4)

$$K_c = Y \cdot \sigma_c \sqrt{\pi a_c} \tag{4}$$

where Y is a dimensionless geometric factor and σ_c is the critical fracture strength (MPa). Materials with high K_c can withstand higher thermal or mechanical loads.

Conventional fracture toughness tests are conducted on large specimens with fatigue crack introduced into them so to create as close as possible conditions to those defined by the linear elastic fracture mechanics (LEFM) [32, 33]. This means that the plasticity at the crack front and tri-axiality are limited (small-scale yield conditions) due to the restraining volume of the specimen. ASTM E 399 [34] standard states five types of specimens and loading setups that stand in these conditions. In the test itself, the specimen is subjected to tensile or flexural loading up to fracture while the load and crack opening displacement (COD) [16] are recorded. After the test concluded, the recordings are postprocessed by the method given in the ASTM standard in order to evaluate the fracture toughness of the material. After writing that, most of the TE material nowadays suffer from low-volume fabrication, and specimens adequate with ASTM E 399 could not be machined. Therefore, most of the published data of fracture toughness were measured by different methods—the ***Vickers Indentation Hardness***, ***Chevron Notch Flexure*** (detailed in ASTM C 1421 [35]), and recently a growing number of reports where ***nano-indentation*** had been used [19–22]. Another method, which was never utilized with TE materials, is the ***Chevron Notch Fracture Toughness*** (also known as the short rod) [36].

2.4.1. Vickers indentation hardness as a measure of the fracture toughness

In the case of ceramics and other materials with a brittle nature where fabrication is hard or costly, an emerging test method is based on the evaluation of the fracture toughness using the Vickers Indentation Hardness test through the cracking at the indentation edges. First

http://dx.doi.org/10.5772/intechopen.75476

suggested by Swain and Lawn [37], a general equation relating the hardness and fracture toughness is in the form described in Eq. (5)

$$K_R = \xi \left(\frac{E}{H}\right)^n P C_0^{-3/2} \quad (5)$$

where K_R is the fracture toughness (Pa·√m); ξ, dimensionless material constant which describes its resistance to crack propagation; E, Young's modulus (Pa); H, Vickers hardness number (Pa); P, the load applied in the hardness test (Pa); C_0, half of the surface crack length (m); n, equation constant which is dependent on the data fitting of the results (0.4–0.5).

This common, cheap, and easy testing method requires only slightly different result interpretation procedure compared to measuring Vickers Hardness number alone. Furthermore, much of the values reported in the study for TE materials were obtained by this technique and can be compared. The disadvantages are the large standard deviation in the results (which can be corrected while using large sample size) and the uncertainty in the fracture mechanisms for each material which results in diverse experimental equations for K_{IC} [38]. The two known crack shapes upon fracture under the Vickers indent are the ***Median*** (half-penny) and ***Palmqvist*** [38] (see **Figure 3**). The median type suggests that the surface cracks from the hardness indentation are interconnected in the specimen depth, while in the Palmqvist type, each crack is independent. It is common to differentiate between the two shapes by measuring the ratio between the crack's length (2c) and the indent's diagonal (2a). If the ratio is larger than 2, it is common to relate it to the median shape, else it is Palmqvist. So far in the study, most of the equations that correlate hardness with fracture toughness are based on a numerical fitting of experimental data and are material-dependent. A short list of such equations is described in **Table 2**. The decision of which equation is the most appropriate upon developing of new materials is to be made with much care. One should be aware of the different equations offered based on their origin and the nature of cracking in the tested material (median or Palmqvist). As up to date, there is no sufficient data and comparison between values obtained by this test method and others for any given material to conform and favor one equation over the others. One reported comparison between the three methods for evaluating the fracture toughness of skutterudites [39] has found that this technique is inadequate in a comparison to the Chevron Notch Flexure method.

Fracture toughness of several common TE materials (such as Bi_2Te_3 and GeTe) tested by this test method showed values in the range of ~0.4–1 MPa√m [1, 13], while $Si_{0.8}Ge_{0.2}$ showed a fracture toughness of ~1.6 MPa√m [12] and the highest reported value is of 1.7 MPa√m for $Yb_{0.35}Co_4Sb_{12}$ [15].

2.4.2. Nanoindentation

Nano-indentation utilizes atomic force microscope (AFM) to basically perform a hardness test. The system records the depth of the indenter as a response to a very small load (up to about 1000 mN) applied over a small contact area size (at the range of few nm^2), resulting in a load-displacement curve, where the displacement is the penetration depth of the indenter into the material. Following the test, the indentation geometry is also measured and evaluated as a complementary data. This means that nano-indentation can be used to evaluate all of the abovementioned mechanical properties, starting with the elastic ***Young's modulus***, going

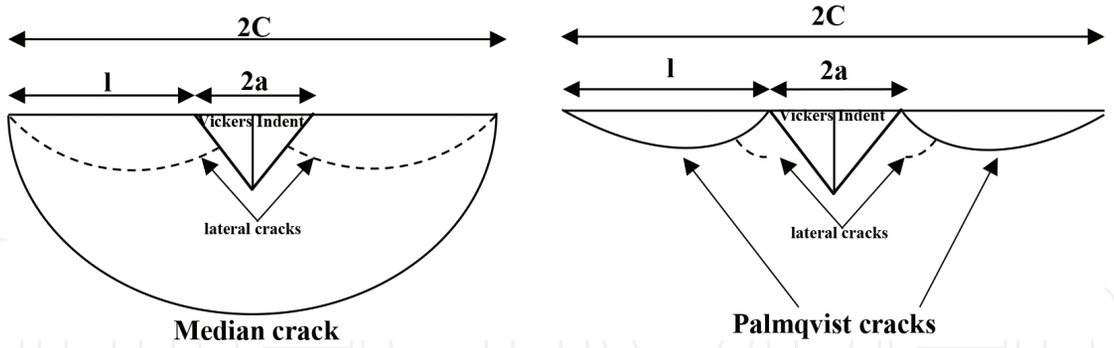


Figure 3. A schematic representation of median and Palmqvist cracks.

#	Equation	Crack type	Reference
1	$K_{IC} = 0.016\left(\frac{E}{H_V}\right)^{1/2}\frac{P}{C^{3/2}}$	Median	[40]
2	$K_{IC} = 0.0752\frac{P}{C^{3/2}}$	Median	[41]
3	$K_{IC} = 0.0089\left(\frac{E}{H_V}\right)^{2/5}\left(\frac{P}{a\,C^{1/2}}\right)$	Palmqvist	[42]
4	$K_{IC} = 0.0319\frac{P}{a\,C_0^{1/2}}$	Palmqvist	[43]

Table 2. Hardness and fracture toughness relations.

through the **yield** *and* **ultimate stresses,** and up to ***hardness*** and ***fracture toughness***. Due to the small sampling area, this technique is ideal for the measurement of materials with low fabrication volumes and such that consist micro- or sub-micron features in their structure (as in the case of many of the recently developed TE materials). In spite of these advantages, the small measured area possesses a major limitation due to the fact that in order to evaluate the macroscopic properties of the material, it is paramount to make a large number of measurements to eliminate any micro-feature dependence and to acquire the average macroscopic property. Furthermore, AFM testing systems are not available for any material's manufacturer and not even at any research center. AFM should be operated by an experienced and educated man power in order to acquire believable results (with low values of uncertainties and errors [44]) and to reduce the wearing of the system, which is quite expensive to maintain (mainly due to indenters' high fabrication costs). For further reading and understanding of nano-indentation, the reader may read the following reference [21].

Several TE materials were evaluated by this testing method and reported recently, such as $Ba_8Al_{15}Si_{31}$ [19] which was reported to have Young's modulus of 109.7 GPa (about 10% higher than the value calculated from time-of-flight measurements) and Vickers hardness of 634 HV which is in a good agreement to the micro-hardness value. Also, *p*- and *n*-type half-Haussler [19] compositions showed Young's modulus of 221 and 186 GPa and a hardness of 12.8 and 9.1 GPa, respectively. Other materials that were measured by this technique can be found in [17]. Although reports using this technique can be found with an increasing amount over the years, it was rarely applied for fracture toughness assessment as was recently applied for Bi_3Se_2Te with Young's modulus of 197.2 GPa, a hardness of 5.6 GPa, and a fracture toughness of 2.4–2.6 MPa√m [32].

2.4.3. Chevron notch fracture toughness (short rod)

This method, first introduced by Barker in 1977 [36] and more recently standardized in ASTM B 771 [45], measures the fracture toughness of both ductile and brittle materials using a Chevron Notch rod-type specimen subjected to tension loading. The specimen is loaded until a small load drop is recorded, indicating an initiation and propagation of a crack well prior to a catastrophic fracture. The ASTM standard differentiates between smooth growing crack and a discontinuous growing crack, so that ceramics and semiconductors that has some degree of plasticity can be handled as well. After the test is concluded, the recorded data are processed to evaluate the fracture toughness of the material, if all of the validation criteria of the standard are met. This testing method, if carried out correctly, has the advantage of directly measuring the material's fracture toughness, even on miniature-size specimens with the aid of testing jigs and setup such as "Fracjack" [35]. Yet, for obtaining adequate results, the specimen's fabrication must be in a high quality and machining should be made by skilled technicians, due to the fact that the required standard specimen includes many details (see **Figure 4**) and most of the ceramic and semiconducting materials suffer from poor machinability. Furthermore, the results interpretation must be carried out by an experienced man power so that no other errors and uncertainties will affect the calculated results. Up to date, as far as we know, no TE materials tested by this technique were reported. To the authors' best experience, such a test method could provide the most accurate fracture toughness values of TE materials directly with little uncertainties and without the need to evaluate it from other types of testing and based on data fitting from other material systems, especially if adequate test setup for ultra-small-sized samples is prepared.

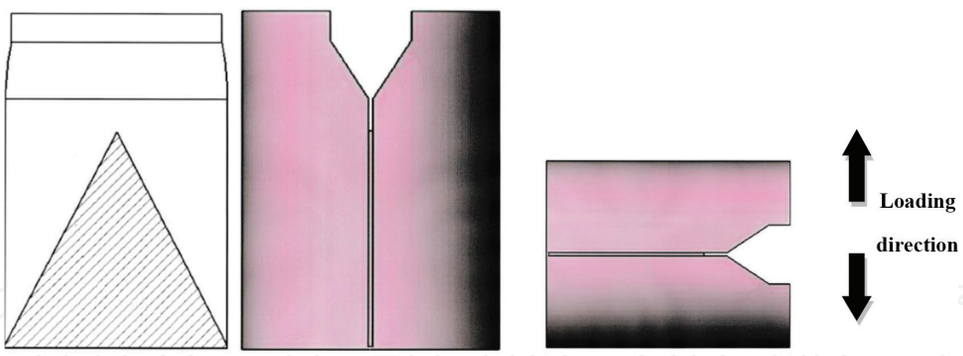


Figure 4. Short-rod specimen geometry and loading setup.

2.5. Thermal shock and fatigue

Due to the fact that TE service conditions include thermal cycles, it is also highly important that such materials will have thermal shock and fatigue resistance. *Thermal shock resistance* is the material's ability to adhere the thermal stresses introduced into it by a sudden increase in temperature as can be calculated by Eq. (6)

$$\sigma_{thermal} = \alpha E \Delta T \tag{6}$$

where $\sigma_{thermal}$ is the thermal stress (Pa), α is the coefficient of thermal expansion (CTE) (1/k), E is Young's modulus (Pa), and ΔT is the temperature difference on the material (k).

For the case where the thermal stress is lower than the yield/fracture stress, then the material will sustain the shock. Therefore, thermal shock could be connected and evaluated via other material's mechanical properties such as Young's modulus, Poisson's ratio, and fracture stress and other thermal properties based on the thermoelastic approach as being expressed in Eq. (7)

$$R' = \frac{\sigma_f(1-\nu)\kappa}{\alpha E} \tag{7}$$

where R' is the thermal shock resistance (W/m), σ_f is the material's fracture stress (Pa), ν is Poisson's ratio, and κ is the total thermal conductivity (W/m·k). The higher the R' value, the greater the resistance.

Thermal fatigue is the material's capability to adhere to multiple cycles of heating and cooling. As the material is capable to withstand higher number of cycles, it is said that it has a higher thermal fatigue resistance. The only way to measure this property is currently to subject such a material to thermal cycles and to evaluate its consistency every few cycles.

As of the current time, according to our knowledge, there are no references in the study concerning these properties with the actual measured values, and the few that mention them do so only in a theoretical fashion as stated earlier.

3. Summary

Mechanical properties of materials represent the material's responses to different loading conditions and are macroscopic representations of the atomic bonding between the atoms from which they are constructed. It was suggested that the cohesive energy (E_C) between two particles can be linked to the elastic constants of the materials and other various physical properties (such as melting temperature, atomic volume, lattice constants, and Debye temperature). Such a correlation opens the possibility of interlinking the material's electronic transport properties with the mechanical ones on the atomic level.

Measuring or evaluating correctly the mechanical properties of TE materials has the potential to bridge between the atomic (mechanical) and physical (electronic/transport) understanding of these materials to the fully developed working modules that will be optimal from both ends standpoint. That way, the material selection for the proper use will be much easier and efficient.

As it was shown in this review, knowing and controlling the mechanical properties of TE materials are paramount necessities for approaching practical TEGs and moving the entire TE technology onward in the Technological Readiness Level (TRL) scale. The material's elastic constants (e.g., Young's modulus and Poisson's ratio), strength, and fracture toughness are the most crucial for the designing practical devices (using finite element analysis). In such an approach, adequate modeling of TEGs could be prepared with lower experimental intervals while saving both money, time, materials, and man power. The elastic constants can provide

the understanding about the material's stiffness, while the strength provides the loading conditions in which the material will maintain its original shape. Knowing the fracture toughness will provide the stress envelope in which the material could operate and its susceptibility to inherent fabrication faults.

Characterizing these mechanical properties (elastic constants, strengths, and fracture toughness) is handful enough and will provide both scientists and manufacturers sufficient data to improve and further proceed to practical TEGs. Characterization methods of these properties are varied with pros and cons to each. It is the authors' opinion to prefer the mechanical methods over the physical ones (such as in the case of Young's modulus measurement by sonic waves), so the results obtained will more accurately describe the material's response to mechanical loading. In evaluating the material's strength, it will be best to choose the type of testing method in which the loading conditions are as close as possible to the expected service conditions of the material. In order to establish a coherent database for all of the developed materials, it will be adequate to test all of these materials under compression and flexural conditions. This is due to the fact that most of the currently available published were obtained following compression conditions, and for the reason, flexure conditions are more susceptible to defect in the material. For measuring fracture toughness, it seems to be wise to choose other testing methods than the Vickers Indentation Fracture, which is prone to errors and uncertainties. It may be applied for a qualitative evaluation of the property as required for distinguishing between fabrication parameters, but for quantitative modeling and calculations, it will be better to use the testing method reported in the standards such as ASTM C 1421 [36] and ASTM B 771 [36].

The abovementioned mechanical properties are not the only mechanical properties at question but also the major ones that should to be evaluated. A more detailed mechanical design will require also the characterization of the fatigue limit and thermal fatigue resistance depending on the expected service conditions of the developed practical TE devices.

Acknowledgements

The authors would like to thank the Ministry of National Infrastructures, Energy and Water Resources for granting this project, grant no. 215-11-022.

Author details

Gilad M. Guttmann[1]* and Yaniv Gelbstein[2]

*Address all correspondence to: gilad.guttmann@gmail.com

1 Department of Materials Engineering, Nuclear Research Center Negev, Beer-Sheva, Israel

2 Department of Materials Engineering, Ben-Gurion University of the Negev, Beer-Sheva, Israel

References

[1] Liu W, Jie Q, Kim HS, Materialia R-Z. Current progress and future challenges in thermoelectric power generation: From materials to devices. Acta Materialia. 2015

[2] Snyder G, Toberer E. Complex thermoelectric materials. Nature Materials. 2008;**7**(2): 105-114

[3] Wacke S, Górecki T, Górecki C, Książek K. Relations between the cohesive energy, atomic volume, bulk modulus and sound velocity in metals. Journal of Physics Conference Series. 2011;**289**(1):012020

[4] Ren F, Case ED, Timm EJ, Lara-Curzio E, Trejo RM. Anomalous temperature-dependent Young's modulus of a cast LAST (Pb–Sb–Ag–Te) thermoelectric material. Acta Materialia. 2010;**58**(1):31-38

[5] Barako M, Park W, Marconnet A, Asheghi M, Goodson K. Thermal cycling, mechanical degradation, and the effective figure of merit of a thermoelectric module. Journal of Electronic Materials. 2013;**42**(3):372-381

[6] Ziabari A, Suhir E, Shakouri A. Minimizing thermally induced interfacial shearing stress in a thermoelectric module with low fractional area coverage. Microelectronics Journal. 2014;**45**(5):547-553

[7] Liao L-L, Dai M-J, Liu C-K, Chiang K-N. Thermo-electric finite element analysis and characteristic of thermoelectric generator with intermetallic compound. Microelectronic Engineering. 2014;**120**:194-199

[8] Mansouri N, Timm E, Schock H, Sahoo D, Kotrba A. Development of a circular thermoelectric Skutterudite couple using compression technology. Journal of Energy Resources Technology. 2016;**138**(5):052003

[9] Ur S-C, Nash P, Schwarz R. Mechanical and thermoelectric properties of Zn4Sb3 and Zn4Sb3+Zn directly synthesized using elemental powders. Metals and Materials International. 2005;**11**(6):435-441

[10] Kallel AC, Roux G, Martin CL. Thermoelectric and mechanical properties of a hot pressed nanostructured n-type Si80Ge20 alloy. Materials Science and Engineering. 2013; **564**:65-70

[11] Bathula S, Jayasimhadri M, Dhar A. Mechanical properties and microstructure of spark plasma sintered nanostructured p-type SiGe thermoelectric alloys. Materials and Design. 2015;**87**:414-420

[12] Zhao L-D, Zhang B-P, Li J-F, Zhou M, Liu W-S, Liu J. Thermoelectric and mechanical properties of nano-SiC-dispersed Bi2Te3 fabricated by mechanical alloying and spark plasma sintering. Journal of Alloys and Compounds. 2008;**455**(1-2):259-264

[13] Schmidt R, Fan X, Case E, Sarac P. Mechanical properties of Mg2Si thermoelectric materials with the addition of 0-4 vol% silicon carbide nanoparticles (SiCNP). Journal of Materials Science. 2015;**50**(11):4034-4046

[14] Case ED. Thermomechanical Properties of Thermoelectric Materials. Boca Raton, FL: CRC Press; 2012

[15] Kenfaui D, Chateigner D, Gomina M, Noudem J. Texture, mechanical and thermoelectric properties of Ca3Co4O9 ceramics. Journal of Alloys and Compounds. 2010; **490**(1-2):472-479

[16] Ravi V, Firdosy S, Caillat T, Conference L-B. Mechanical properties of thermoelectric skutterudites. AIP Conference. 2008

[17] Le P, Luo C-W, Jian S-R, Lin T-C, Yang P-F. Nanomechanical properties and fracture toughness of Bi3Se2Te thin films grown using pulsed laser deposition. Materials Chemistry and Physics. 2016;**182**:72-76

[18] Tasi C-H, Tseng Y-C, Jian S-R, Liao Y-Y, Lin C-M, Yang P-F, et al. Nanomechanical properties of Bi2Te3 thin films by nanoindentation. Journal of Alloys and Compounds. 2015;**619**:834-838

[19] He R, Gahlawat S, Guo C, Chen S, Dahal T, Zhang H, et al. Studies on mechanical properties of thermoelectric materials by nanoindentation. Physica Status Solidi. 2015; **212**(10):2191-2195

[20] Li G, Gadelrab K, Souier T, Potapov P, Chen G, Chiesa M. Mechanical properties of BixSb2−xTe3 nanostructured thermoelectric material. Nanotechnology. Nanotechnology. 2012;**23**(6):065703

[21] Anno H, Ueda T, Hirata S, Kameyama T, Iida T, Kogo Y. Mechanical properties of thermoelectric Ba8Al15Si31 Clathrate prepared by combining arc melting and spark plasma sintering techniques. Journal of Electronic Materials. 2016;**45**(3):1803-1812

[22] Gelbstein Y, Tunbridge J, Dixon R, Reece M, Ning H, Gilchrist R, et al. Physical, mechanical, and structural properties of highly efficient nanostructured n- and p-Silicides for practical thermoelectric applications. Journal of Electronic Materials. 2014;**43**(6):1703-1711

[23] Maynard J. Resonant ultrasound. Spectroscopy. 1998:132-142

[24] International A. ASTM D2845: Standard Test Method for Laboratory Determination of Pulse Velocities and Ultrasonic Elastic Constants of Rock. ASTM International; 2008

[25] Aksel C, Riley F. Young's modulus measurements of magnesia–spinel composites using load–deflection curves, sonic modulus, strain gauges and Rayleigh waves. Journal of the European Ceramic Society. 2003;**23**(16):3089-3096

[26] Plachy T, Pavel, Michal. Comparison of Two Experimental Techniques for Determination of Young's Modulus of Concrete Specimens. In: Cornelia A, Valeri, Emil, Monica, Nikos, editors. Puerto De La Cruz, Tenerife, Canary Islands, Spain: WSEAS Press; 14AD. pp. 68-71

[27] International A. Metals handbook: 01 - properties and selection: Irons, steels, and high-performance alloys. 9th ed. ASM International; 2004

[28] International A. Metals handbook: 02 - properties and selection: Nonferrous alloys and special-purpose materials. 9th ed. ASM International; 2004

[29] Schmidt R, Case E, Zhao L-D, Kanatzidis M. Mechanical properties of low-cost, earth-abundant chalcogenide thermoelectric materials, PbSe and PbS, with additions of 0-4% CdS or ZnS. Journal of Materials Science. 2015;**50**(4):1770-1782

[30] Qian L, Li M, Zhou Z, Yang H, Shi X. Comparison of nano-indentation hardness to microhardness. Surface and Coatings Technology. 2005;**195**(2-3):264-271

[31] Ren F, Case ED, Timm EJ, Schock HJ. Hardness as a function of composition for n-type LAST thermoelectric material. Journal of Alloys and Compounds. 2008;**455**(1-2):340-345

[32] Barker LM. A simplified method for measuring plane strain fracture toughness. Engineering Fracture Mechanics. 1977;**9**(2):361-369

[33] Barker LM. Of and evaluation B-F. Comparisons of fracture toughness measurements by the short rod and ASTM standard method of test for plane-strain fracture toughness of metallic materials (E 399). Journal of Testing and Evaluation. 1980

[34] International A. ASTM E 399: Standard Test Method for Linear- Elastic Plane Strain Fracture Toughness Kic of Metallic Materials. ASTM International; 2012

[35] International A. ASTM C 1421: Standard Test Methods for Determination of Fracture Toughness of Advanced Ceramics at Ambient Temperatures. ASTM International; 2010

[36] International A. ASTM B 771: Standard Test Method for Short Rod Fracture Toughness of Cemented Carbides. ASTM International; 2011

[37] Swain MV, Lawn BR. Indentation fracture in brittle rocks and glasses. International Journal of Rock Mechanics and Mining Science and Geomechanics Abstracts. 1976; **13**(11):311-319

[38] Medeiros EE, Dias A. Experimental and Numerical Analysis of Vickers Hardness Testing

[39] Eilertsen J, Subramanian MA, Kruzic JJ. Fracture toughness of Co4Sb12 and In0.1Co4-Sb12 thermoelectric skutterudites evaluated by three methods. Journal of Alloys and Compounds. 2013;**552**:492-498

[40] Anstis GR, Chantikul P, Lawn BR, Marshall DB. A critical evaluation of indentation techniques for measuring fracture toughness: I, direct crack measurements. Journal of the American Ceramic Society. 1981;**64**(9):533-538

[41] Evans A, Charles E. Fracture toughness determinations by indentation. Journal of the American Ceramic Society. 1976;**59**(7-8):371-372

[42] Niihara K, Morena R. Evaluation of KIc of brittle solids by the indentation method with low crack-to-indent ratios. Journal of Materials Science. 1982

[43] Menčík J. Nanoindentation in Materials Science. 2012

[44] Fischer-Cripps A. Nanoindentation. Springer Science + Busniess Media

[45] Barker LM. Evaluation of a New Fracture Toughness Measuring Technique, and Adaptation of the Technique to Use Ultra-Small Specimens; 1979